Hindawi
Geofluids
Volume 2020, Article ID 8850911, 8 pages
https://doi.org/10.1155/2020/8850911

WILEY | Hindawi

Research Article

A Discussion of Reinforcement Timing Optimization for Main Inclined Shaft Roadway with Water Seepage

Minglei Zhang, Chaoyu Chang, and Wen Cao

Institute of Disaster Prevention, Langfang 065201, China

Correspondence should be addressed to Minglei Zhang; zml@cidp.edu.cn

Received 28 May 2020; Revised 17 July 2020; Accepted 24 July 2020; Published 13 August 2020

Academic Editor: Jingmin Xu

The infiltration and physical and chemical effects of fissure water often have a degrading effect on the strength and bearing capacity of the surrounding rock of the roadway. With the increase of the time of water infiltration, the roadway deformation increases exponentially, resulting in a higher risk of roadway destruction. In this paper, targeting at the supporting and protection issues associated with the main inclined shaft during the water-drenching, a numerical simulation method was established to evaluate the impact of the fissure water on the deformation of the surrounding rock of the roadway, and a solution to control the top water in main inclined shafts by grouting was proposed. Through the numerical simulation method, the effective penetration range of the slurry in the surrounding rock and the variation of the tunnel deformation with the grouting timing were studied. A method of combining numerical simulation with on-site monitoring to determine a reasonable grouting timing was proposed. The field application suggests that grouting at a reasonable timing can effectively control the influence of seepage water from the roof crack of the main inclined shaft on the deformation of the roadway surrounding rock, improve the integrity of the roadway surrounding rock, increase the bearing capacity of the support, and maintain the safety and stability of the roadway surrounding rock of the main inclined shaft. Furthermore, this study can provide insightful references to the grouting reinforcement adopted by similar main inclined shafts.

1. Introduction

With the continuous increase in mining scale and mining intensity, the threat of coal mine roof water hazards has become increasingly prominent, resulting in serious safety hazards to mine production [1, 2]. When the groundwater, as a chemical solution with a complex composition, is exposed to the rocks, complex physical and chemical reactions often occur, resulting in damages to the mechanical properties of the rock mass, such as the softening and hydraulic erosion of rocks. Rock softening is a typical physical property of rock, and the strength deterioration severity depends on the water content of the rock [3]. The hydraulic pressure intensifies the development of the internal cracks in the softened rock mass, gradually reducing the integrity of the rock mass and changing the macromechanical properties of the rock mass [4]. The redistribution of chemical elements caused by water-rock chemistry and changes in rock microstructure further exacerbate the deterioration of rock mechanical properties [5].

During the roadway excavation, with the existences of the fissure water in the surrounding rock, the physical and chemical reactions between the water and the rock mass have a degrading effect on the bear capacity of the roadway surrounding rock, resulting in safety hazards and other risks, which should be either drained or contained effectively to prevent further damage [6]. Under the circumstance that proper drain is not possible, grouting is often adopted to control the fissure water in the roadway surrounding rock and strength the roadway accordingly. Many scholars have conducted in-depth studies on the roadway grouting technologies. In terms of grouting materials, due to the engineering needs and advances in material science, the common materials adopted in the grouting process include cement slurry, loess, fly ash, and other chemical grouting materials [7–10]. In terms of grouting technologies, various grouting methods

are developed such as the adoption of the grouting pipes, grouting anchors, and grouting anchor cables [11–14]. In terms of grouting mechanism, multiple grouting theories have been proposed by different scholars such as porous media grouting, continuous media grouting, and fractured media grouting to study the diffusion law and influencing factors of grouting slurry in rock mass [15–19]. In order to evaluate the strengthening performances of the grouting, article [20] sampled and tested the grouting body mixed with coal and mudstone, respectively. The test results suggest that the residual strengths of the rocks after cement grouting and chemical slurry grouting can be increased by 0.7 to 2 times and 1.5 to 6 times, respectively. According to New Austrian Tunneling Method, the timing to add roadway support should be determined based on "the premium compatibility between the roadway surrounding rock release stress and its self-bearing capacity," which can fully release the deformation energy of the surrounding rock and appropriately reduce the support intensity [21]. Based on New Austrian Tunneling Method, some researchers proposed the timing determination methods of adding primary and secondary support to the deep soft rock roadway, which greatly enriched the surrounding rock grouting reinforcement theory [22–24]. However, the aforementioned studies focus on the single roadway with severe deformation and overlooks the reinforcement needs of the roadway under the influences of the fissure water for an extended period of time. In this paper, studies were conducted to focus on the supporting needed by the roadway of the main inclined shaft. After the analysis to the impacts of the fissure water on the mechanical properties and deformation of the roadway surrounding rock, through the strain and softening structural model included in the FLAC3D numerical simulation software, numerical simulations were established to determine the optimum timing for adding grouting reinforcement to the main inclined shaft. Furthermore, the methods and technical schemes for determining the reasonable grouting timing of the main inclined shaft roadway with fissure water were discussed, which can provide some insightful references for the grouting reinforcement of similar conditions.

2. The Impact of Roof Fissure Water on the Stability of the Roadway Surrounding Rocks

2.1. The Project Overview. The main inclined shaft of the Gucheng has a total length of 2,019 meters with an inclined degree of 15° and a penetration death of 92 meters underground. The fracture surface of the roadway in the bedrock section takes a shape of a straight wall semicircular arch with a width of 6.4 meters and a height of 1.2 meters. The support was constructed with anchor bolts, anchor cables, and sprayed cement. The total thickness of the coated cement is about 200 mm. No water seepage is founded in the surface soil layer of the main inclined shaft. On the other hand, in the bedrock section, due to the skip of determining the water contents and proper draining, water seepage occurred during the layout of the anchor cables. Water seepage was observed in the bolt holes. Some bolt holes suffered with severe water seepage, as well as the surrounding area of the roof displacement monitors. The severe water seepage has jeopardized the support effects of the roadway and field construction. In order to ensure the construction progress, no more anchor bolt hole is drilled at the point of 580 meters. Instead, anchor mesh and coating cement were installed. No anchor cable was installed from 580 meters to 880 meters. Anchor cables were installed after 880 meters. The supporting parameters of the roadway section with water seepage and the appearances of the roadway are provided in Figures 1 and 2 below.

Underground water is a complexed chemical solution. Under the interaction between the underground water and the rock, the physical and chemical properties of the rock tend to change including the macrostructure and the increased porosity, resulting in severe damages to the rock. Simultaneously, the increasement of the permeability and the water pressure at the pores lower the effective stress of the rock, resulting in lower resistances of the surrounding rocks to the deformation. The macrostrength and the rigidity of the surrounding rock are further reduced accordingly. On the other hand, under the pressure of the infiltration water, the underground water enters the roadway surrounding rock through the fissures developed dynamically and weakens the bear capacity of the surrounding rock and the supporting structure, resulting in failure of the bolting structure and safety hazards. From the long-term perspective, the underground water poses as a threat to the supporting structure, especially to the metal anchor bolts and cables such as the rust and erosion, increasing the failure risks of the supporting structure and jeopardizing the safety of the main inclined shaft.

2.2. The Numerical Simulation of the Roadway Surrounding Rock Deformation. FLAC3D numerical simulation software was adopted to build model to evaluate the impact of the water seepage to the deformation of the roadway surrounding rock. The model was built based on the rock layer distribution, and the physical properties of the main inclined shaft obtained from the Gucheng coal mine. The parameters of the rock layers are presented in Table 1 below. The size of the model is $300 \times 100 \times 40$ m. The rock damage is estimated based on the Mohr-Coulomb criterion and the strain-softening model. 2.58 MPa was applied to the top part of the model with no restriction applied. Restrictions were applied to both the left side and right side of the model. A perpendicular restriction was applied to the bottom of the model. According to relevant studies, the roadway with water seepage was divided into two conditions including the roadway with the short-term seepage (grouting was added within half a year after the construction) and the roadway with long-term seepage (no grouting after the construction). Strength reduction was used to indicate the damage to the roadway strength, until the strength was reduced to the 80% and 50% of the initial roadway strength [25].

Figure 3 shows the roadway displacement distribution and statistics. Under normal circumstances, the main inclined shaft roadway demands more to the deformation control of the surrounding rock with a higher level of the support, which often leads to limited roadway deformation. Comparing with regular roadway, both the bottom and top deformations of the

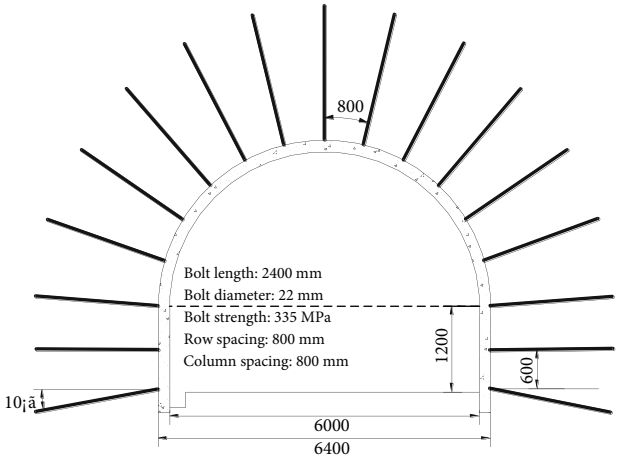

Figure 1: The supporting parameters and appearance of the roadway.

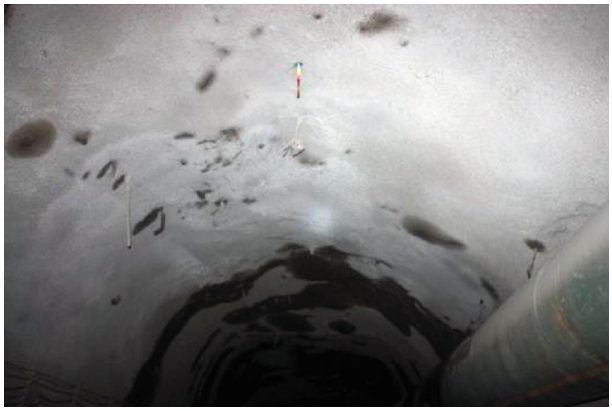

Figure 2: Roadway appearance (without anchor cable).

roadway exposed to the short-term water seepage were increased by 2.63 times and 4.07 times for the lateral deformation. In contrast, both the bottom and top deformations of the roadway exposed to the long-term water seepage were increased by 11.8 times and 12.7 times for the lateral deformation. The test indicates that the short-term water seepage has a limited impact on the roadway strength. However, the long-term water seepage can severely degrade the roadway strength. Most of the main inclined shaft often have a long service life, as long as 50 to 60 years. The negative impact of the water seepage on the strength of the roadway is mostly likely to occur and last for an extended period of time, demanding effective measures to control the water seepage in the roadway.

No major strata behavior was noticed within a short period of time. However, the main inclined shaft located at the Gucheng coal mine is required to have a long service life, demanding a high level of support. The anchor cables play a vital role in the supporting system of the main inclined shaft. During the survey, a large amount of mudstone with low strength were detected, which can easily crack during the excavation due to the original stress of the rocks. The cracks will allow the water seepage developed, jeopardizing the supporting, and the construction progress. Often, the preferred solution is to drain the water from the roof. However, due to the large amount of water and tight schedule, the support of combining the grouting and the anchor cables were selected for the roof section with water seepage of the main inclined shaft.

3. The Numerical Simulation of the Timing to Grout in the Roadway Section with Water Seepage of the Main Inclined Shaft

The grouting timing refers to the time interval between the second support of the grouting anchor cable and the installation of the anchor bolts and the sprayed cement. The field experiences suggest that newly excavated roadway is not suitable to grout within a few days after the excavation. After the excavation, the roadway is still in the process of stress distribution, exposing the surrounding rock to the easy development of the damage and deformation. If the grouting is conducted too early, the fissures are too small to accept the grouting. Also, the continuous release of the stress and deformation of the surrounding rock can possibly damage the solidified grouting. If the grouting is conducted too late, the deformation of the surrounding rock has been developed excessively. Despite the good diffusion of the grouting slurry in the fissures, the surrounding rock has lost its bear capacity, resulting in a limited effect of reinforcement. Therefore, a good timing for the grouting is critical for the effectiveness of the supporting system.

3.1. The Impact of the Grouting Time on the Thickness and Stability of Effective Permeation Circle of Grouting Slurry in Surrounding Rock. Essentially speaking, the deformation of the surrounding rock is a process of stress release and transfer, as well as a strength reduction process. The grouting is designed to solidify the broken and fractured rocks after the peak. FLAC3D numerical simulation software was adopted to simulate the solidifying process of the grouting of the roadway with water seepage. A strain and softening model is used to simulate the after peak damage suffered by the rock [26, 27]. The fracture degree of the rock after the peak is indicated with equivalent plastic shear strain [28–30]. As the equivalent plastic shear strain increased, the rock strength after the peak reduced drastically. The general cohesion was reduced significantly, while the general fraction angles experienced less changes. Assuming that the grouting was carried out when the rocks were still in the process of fracture development, the grounding can spread to the fracture areas of the rock, achieving a highly effective permeation status. The fracture area achieved effective permeation status is labeled as an effective permeation circle. To evaluate the impact of grouting timing on the solidifying effect of the grouting, the grouting was carried out at the following equivalent plastic shear strain including 0.01, 0.08, 0.16, 0.24, 0.32, 0.40, 0.48, 0.56, 0.64, and 0.72. Considering that different damage levels in various locations within the rock, the maximum value in the fracture area was selected as the equivalent plastic shear strain. The impacts of the grouting time on the effective permeation circles of grouting slurry,

Table 1: The physical parameters of the rock layers.

Rock layer	Thickness/m	Density/kg.m^3	Bulk Modulus/GPa	Shear Modulus/GPa	Tensile strength/MPa	Cohesion/MPa	Internal friction angle/°
Overlying rock	30	2300	2.65	1.47	3.81	4.69	32
Sandstone	4	2350	16.24	11.15	4.69	6.79	35
Mudstone	3.5	2150	2.32	1.09	1.81	2.19	30
Sandstone	2.5	2350	16.24	11.15	4.69	6.79	35
Mudstone	5	2150	2.32	1.09	1.81	2.19	30
Sandy mudstone	6.5	2300	2.66	1.46	2.11	2.49	33
Mudstone	13.5	2150	2.32	1.09	1.81	2.19	30
Siltstone	3	2450	15.72	9.81	3.62	5.91	33
Mudstone	2	2150	2.32	1.09	1.81	2.19	30
Underlying bed	30	2300	2.65	1.47	3.81	4.69	32

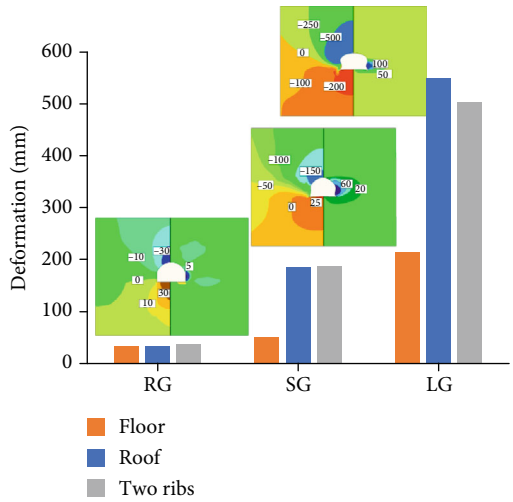

Figure 3: The roadway displacement distribution and statistics (RG represents for routine group, SG represents for short-term water seepage group, and LG represents for long-term water seepage group).

the deformation, and the damage were analyzed through the calculation. In the numerical simulation, the internal cohesion and the internal fraction angles were increased to simulate the grouting effect. According to the relevant researches, the strength of grouted rocks was assumed as 1.8 times of that before the grouting.

The flow and penetration range of the slurry in the surrounding rock depends on the crack development within the surrounding rock. Therefore, the grouting performed differently under different damage states after the peak and so was the effective penetration range of the slurry. Meanwhile, due to the different fracture state of the surrounding rock during grouting, the residual strengths of the rock in the effective grouting circle varied, affecting the strength of grouting and resulting in different reinforcement effects to the roadway surrounding rock. Figure 4 shows the distribution characteristics of the grouting slurry effective permeation circle in the surrounding rock under different grouting timings. The thickness of the slurry effective permeation circle and the deformation of the roadway surrounding rock at various grouting timings are presented in Figure 4 as well.

The simulation results indicate that the permeation range of the grouting slurry was increased along with the delay of the grouting. At the early fracture stage, the increasing of the equivalent plastic shear strain led to the fast development of the fractures, resulting in more fracture space. The thickness of the slurry effective permeation circle was increased from 0.3 m to 1.4 m. At the middle fracture stage, the fracture space increased at a lower rate. The thickness of the slurry effective permeation circle was increased from 1.4 m to 2.8 m. At the residual deformation stage of the surrounding rock, the stress redistribution was complete, and the fracture area expanded slowly, resulting in a stable thickness of slurry effective permeation circle. The thickness of the slurry effective permeation circle stands for the permeation and diffusion effect of the grouting slurry. A higher thickness of the slurry effective permeation circle indicates a wider range of permeation and diffusion of the grouting slurry. However, the range of grouting slurry permeation and diffusion is not the sole deciding factor in the strength of the slurry solidification, which also depends on the strength of the surrounding rock during the grouting process. Normally, a higher strength of the surrounding rock during the grouting process leads to a stronger grouting body. An early grouting timing leads to a smaller range of permeation and diffusion and a stronger grouting body. On the other hand, a delayed grouting timing leads to a wider range of permeation and diffusion and a weaker grouting body. Therefore, a turning point was observed in the deformation curve of the roadway surrounding rock corresponding to the grouting time. A U shape was developed as the grouting timing was postponed, suggesting a reduction followed by an increase in the deformation of the roadway surrounding rock. This change suggests that an optimum timing range does exist to strive for a balance between the effective permeation range and the strength of the grouting slurry, resulting in an effective control to the deformation of the roadway surrounding rock.

3.2. The Determination of the Optimum Support. Based on the analysis mentioned above, the optimum grouting timing

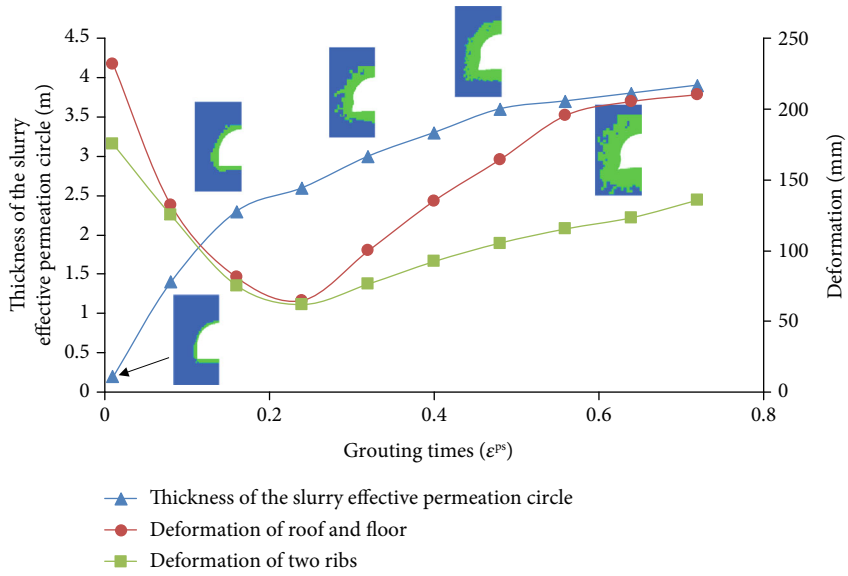

Figure 4: The thickness of the slurry effective permeation circle and the deformation of the roadway surrounding rock at various grouting timings.

is between 0.16 and 0.32 ($\varepsilon^{ps} = 0.16 \sim 0.32$). However, the maximum equivalent plastic shear strain could not be obtained from the field measurement. The roadway deformation can be measured easily, which is a frequently needed parameter in the field, which can be used as an indicator to determine the grouting timing of the roadway. According to the simulation results, when the maximum equivalent plastic shear strain of the surrounding rock is between 0.16 and 0.32 ($0.16 < \varepsilon^{ps} \leq 0.32$), the roadway roof deformation (U_r), the lateral deformation (U_l), and the bottom deformation (U_f) were $48.5\,\text{mm} < U_r \leq 65.2\,\text{mm}$, $54.8\,\text{mm} < U_l \leq 70.6\,\text{mm}$, and $12.1\,\text{mm} < U_f \leq 15.4\,\text{mm}$, respectively, suggesting an optimum timing range for grouting.

During the field application, the specific engineering geological conditions should be included to obtain the roadway surface deformation corresponding to the best grouting timing of the roadway, followed by the field monitoring of the deformation of the roadway surrounding rock. When the deformation of the roadway surrounding rock reaches the deformation corresponding to the optimum grouting timing, the grouting should be carried out.

4. The Field Application and Reinforcement Effect

According to the analysis above and the filed monitoring to the roadway deformation of the main inclined shaft, grouting should be conducted 4 to 5 months after the excavation to achieve the effective control to the roadway deformation. Without disruption to the construction progress, the main inclined shaft should be reinforced with the anchor bolts and the sprayed concrete. The secondary reinforcement should be added 4 months after the excavation by the adoption of the latest hollow grouting anchor cables which was fabricated with eight wound 7 mm-diameter metal tubes.

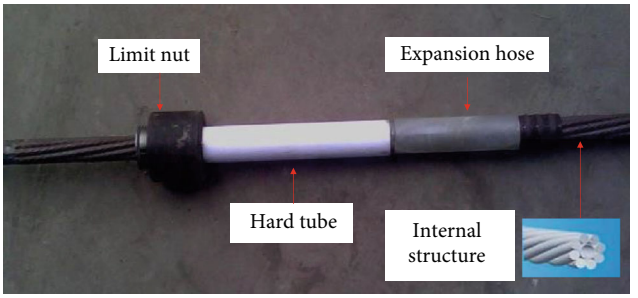

Figure 5: Grouting cable anchor.

The sealing package includes seal clamps, expandable flexible hoses, and hard plastic tubes.

The dimension of the hollow grouting anchor cable is 8300 mm at length and 22 mm at diameter, as shown in Figure 5. Each row was installed with three grouting anchor cables with a distance of 2000×1600 mm in-between. The sprayed slurry was mainly cement (#42.5 standard Portland cement with a water and ash ratio of 1 : 1.5). ACZ-1 agent was also added to the slurry, which contains 8% cement. The sealing clamp has been assembled on the anchor cable body when the anchor cable was delivered from the factory. When installing the anchor cable, the expansion soft rubber tube shall be sleeved first, and then, the plastic hard tube shall be sleeved. It shall be confirmed that the hard tube is 50-80 mm away from the hole opening. After that, the plastic hard tube shall be pushed through the special pushing device, until the soft rubber tube can be pressurized and expanded to seal the hole. The layout of grouting cable anchor is shown in Figure 6. Before grouting, multiple prayed cement spots had been permeated with water. After the installation of the grouting anchor cables, fissure water was drained along the anchor cable holes, as demonstrated in Figure 7. After the grouting, the fissure water migrated beyond the area of the grouting area

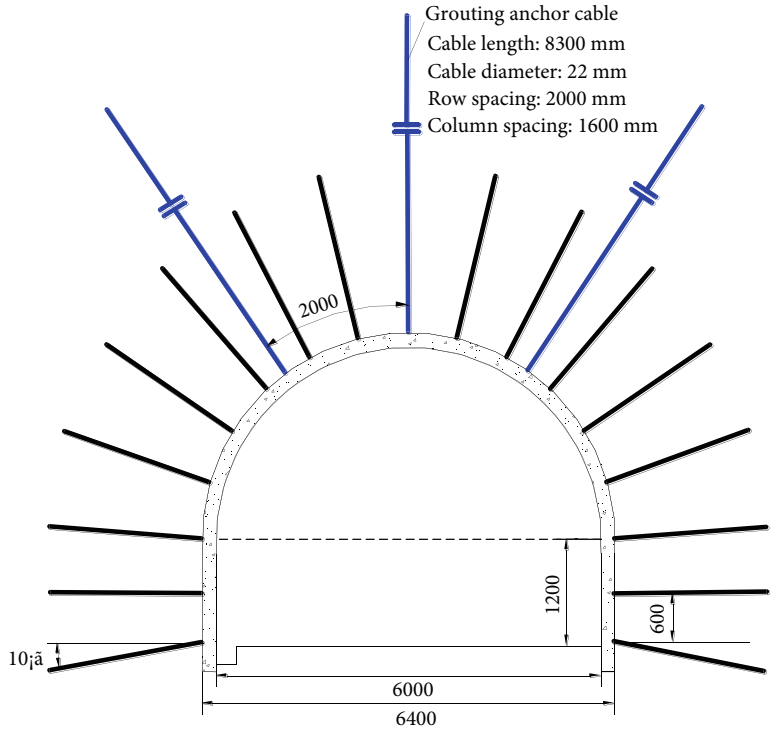

Figure 6: Layout of grouting cable anchor.

Left (before grouting) Middle (before grouting) Right (before grouting)

Left (after grouting) Middle (after grouting) Right (after grouting)

Figure 7: Comparison of water flow in anchor hole before and after grouting.

and no more water seepage was detected. After a while, the permeated water in the sprayed cement was evaporated, and no water seepage was observed visually, as demonstrated in Figure 8.

As shown in Figure 9, the maximum deposition in roof was 8 mm with a maximum of 6 mm bulging at the bottom. The roof displacement was about 14 mm. The roof deposition was slightly higher than the bulging at the bottom; which suggests that due to the roof fissures under the water impact, the roof rock was weakened, resulting in more deposition than the bottom. The maximum displacements of the roadway at the left and right were 4 mm and 7 mm, respectively.

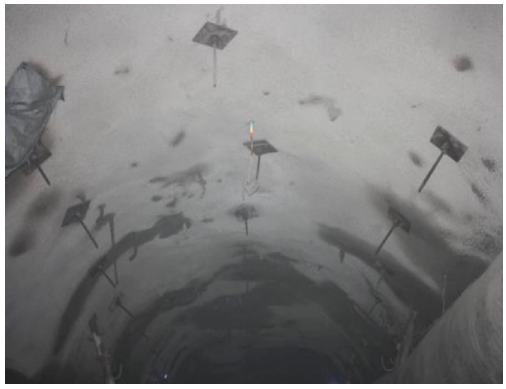

Figure 8: Grouting effect.

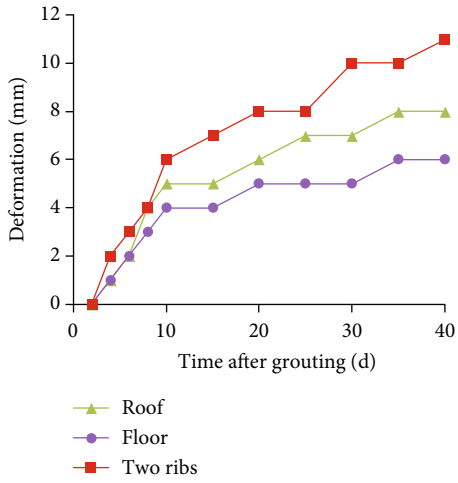

Figure 9: The roadway deformation after grouting.

The total lateral displacement reached a total of 11 mm. The limited roadway deformation occurred 9 days after the installation of the grouting anchor cables, suggesting that a quality reinforcement provided by the grouting anchor cables to the roadway roof.

5. Conclusion

(1) The permeation effect and the physical and chemical effect of the flowing water tend to degrade the strength of the roadway surrounding rock and bear capacity. The degrading effect increases exponentially as the water penetration extends, resulting in the increased risks of roadway failures

(2) The effective permeation range increases as the grouting timing delays, but not the strength of the grouting body, which leads to the decreasing of the roadway deformation, followed by the increasing deformation. Therefore, an optimum grouting timing should be selected to achieve a preferred grouting slurry permeation range and the strength of the grouting body, resulting in effective control of the surrounding rock deformation

(3) Combining the numeric simulation and the field monitoring, a grouting timing determination method based on the surrounding rock deformation of the roadway is proposed for the main inclined shaft. The field application demonstrates a proper grouting time can effectively control the roof fissure water permeation effect on the deformation of the roadway surrounding rock in the main inclined shaft, improve the integrity of the roadway surrounding rock, increase the bearing capacity of the supporting structure, and maintain the safety and stability of the roadway surrounding rock of the main inclined shaft

Data Availability

The data used to support the findings of this study are available from the corresponding author upon request.

Conflicts of Interest

The authors declare that there is no conflict of interest regarding the publication of this paper.

Acknowledgments

This work is supported by the Fundamental Research Funds for the Central Universities (grant no. ZY20200203), the Key tasks for earthquake emergency youth of China Seismological Bureau (CEA_EDEM-202029), and Self financing project of scientific research and development plan of Langfang science and Technology Bureau (grant no. 2020013046).

References

[1] Q. Wu, M. Wang, and X. Wu, "Investigations of groundwater bursting into coal mine seam floors from fault zones," *International Journal of Rock Mechanics and Mining Sciences*, vol. 41, no. 4, pp. 557–571, 2004.

[2] Y. Zhang, S. Cao, N. Zhang, and C. Zhao, "The application of short-wall block backfill mining to preserve surface water resources in northwest China," *Journal of Cleaner Production*, vol. 261, article 121232, 2020.

[3] C. Y. Zhou, N. Liang, and Z. Liu, "Multifractal characteristics of pore structure of red beds soft rock at different saturations," *Journal of Engineering Geology*, vol. 28, no. 1, pp. 1–9, 2020.

[4] Z. Zhang, H. Cao, T. Y. Wang, and Z. L. Ni, "Experimental investigation on swelling inhibition of shale in northwestern Hunan under the interaction of shale-fluid," *Bulletin of Science and Technology*, vol. 35, no. 12, pp. 6–11, 2019.

[5] Y. P. Xie, Q. N. Chen, X. C. Huang, and P. Luo, "An experimental study of microstructure and uniaxial compression test of carbonaceous slate in a deep buried tunnel," *Hydrogeology and Engineering Geology*, vol. 47, no. 1, pp. 96–102, 2020.

[6] Z. J. Gao, J. T. Liu, Y. Z. Li et al., "Hydro chemical characteristics and hydrogeochemical simulation of pore groundwater in Lhasa valley area," *Journal of Shandong University of Science and Technology (Natural Science)*, vol. 39, no. 1, pp. 1–10, 2020.

[7] T. F. Gu, Z. D. Sun, F. T. Luo, Y. M. Liu, K. Guo, and L. Feng, "Experimental research on loess grouting material for coal gob

filling," *Journal of Engineering Geology*, vol. 22, no. 1, pp. 98–105, 2014.

[8] G. C. Yan, L. J. Bai, Z. Q. Zhang, T. Yang, and J. H. Liu, "Experimental and applied study on PU modified chloroaluminate cement grouting material," *Journal of China Coal Society*, pp. 1–7, 2020.

[9] H. Liang, L. Fan, H. Wei, and Y. Z. Li, "Study on influencing factors of strength of polyether polyurethane grouting material," *Journal of Wuhan University of Technology*, vol. 44, no. 1, pp. 172–176, 2020.

[10] X. M. Guan, H. B. Zhang, Z. P. Yang et al., "Research of high-performance inorganic-organic composite grouting materials," *Journal of China Coal Society*, vol. 45, no. 3, pp. 902–910, 2020.

[11] S. Y. Guo, "Historic opportunity, development predicament and some suggestions for tunnel and underground works in China," *Tunnel Construction*, vol. 39, no. 10, pp. 1545–1552, 2019.

[12] J. Li, Z. H. Li, and X. D. Hu, "Analysis on water sealing effect of freezing-sealing pipe roof method," *Chinese Journal of Underground Space and Engineering*, vol. 11, no. 3, pp. 751–758, 2015.

[13] Q. Wang, Y. D. Xu, S. Xu, B. Jiang, R. Pan, and B. H. Liu, "Study and application of bolt-grouting slurry diffusion and reinforcement mechanism in broken surrounding rock," *Journal of Mining and Safety Engineering*, vol. 36, no. 5, pp. 916–923, 2019.

[14] G. Y. Wang and L. Jin, "Study on the dynamic response of the tunnel under the action of dynamic load," *Chinese Journal of Applied Mechanics*, vol. 34, no. 5, pp. 881–886, 2017.

[15] Z. L. Zhou, Y. L. Zhao, Z. Chen, X. M. Du, and Z. B. Wu, "Meso-mechanism of compaction grouting in soil based on particle flow method," *Journal of Central South University (Science and Technology)*, vol. 48, no. 2, pp. 465–472, 2017.

[16] L. Wen, Z. Q. Luo, Y. G. Qin, W. Wang, and K. H. Zheng, "Effective diffusion range of exponential fluids based on Navier-stokes equation in collapse area," *Journal of Southwest Jiaotong University*, vol. 55, no. 1, pp. 193–201, 2020.

[17] L. Z. Zhang, Q. S. Zhang, R. T. Liu, and S. C. Li, "Grouting mechanism in fractured rock considering slurry-rock stress coupling effects," *Chinese Journal of Geotechnical Engineering*, vol. 40, no. 11, pp. 2003–2011, 2018.

[18] J. P. Wei, B. H. Yao, Y. Liu, D. K. Wang, P. F. Cui, and S. Yao, "Grouting fluid diffusion law and variable model for fractured coal mass seepage," *Journal of China Coal Society*, vol. 45, no. 1, pp. 201–212, 2020.

[19] Q. Wang, L. Wang, B. H. Liu, B. Jiang, H. J. Zhang, and S. Xu, "Study of void characteristics and mechanical properties of fractured surrounding rock grout," *Journal of China University of Mining and Technology*, vol. 48, no. 6, pp. 1197–1205, 2019.

[20] X. Y. Yu, *Mining Failure Mechanism and Grouting Reconstruction Technology of Coal Wall in the Lag Section of Gob Side Entry*, China University of Mining and Technology, Xuzhou, China, 2014.

[21] S. X. Lei and W. Zhao, "Study on the mechanism of circumferential yielding support for soft rock tunnel with large deformation," *Rock and Soil Mechanics*, vol. 41, no. 3, pp. 1–8, 2020.

[22] K. Wu, Z. S. Shao, and S. Qin, "Investigation on the mechanical behavior of tunnel supported by yielding supports in rheological rocks," *Chinese Journal of Theoretical and Applied Mechanics*, vol. 52, no. 3, pp. 890–900, 2020.

[23] Y. Zhang, F. X. Shen, X. M. Sun, M. C. He, J. Wang, and M. Du, "Stress and deformation law of surrounding rock in the second reuse of roadway formed by roof cutting in the "three-soft" coal seam," *Journal of China University of Mining and Technology*, vol. 49, no. 2, pp. 247–254, 2020.

[24] X. Sun, B. Zhang, L. Gan, Z. Tao, and C. Zhao, "Application of constant resistance and large deformation anchor cable in soft rock highway tunnel," *Advances in Civil Engineering*, vol. 2019, Article ID 4347302, 19 pages, 2019.

[25] S. Y. Zhu, S. G. Song, Q. Sun, B. Yan, and C. T. Wang, "Characteristics of interaction process between deep rock of lower coal seam floor and water under different test conditions," *Chinese Journal of Rock Mechanics and Engineering*, vol. 33, Supplement 1, pp. 3231–3237, 2014.

[26] Z. Li, S. Yu, W. Zhu et al., "Dynamic loading induced by the instability of voussoir beam structure during mining below the slope," *International Journal of Rock Mechanics and Mining Sciences*, vol. 132, article 104343, 2020.

[27] Y. Li, C.'. Tang, D. Li, and C. Wu, "A new shear strength criterion of three-dimensional rock joints," *Rock Mechanics and Rock Engineering*, vol. 53, no. 3, pp. 1477–1483, 2020.

[28] Y. L. Lu, L. G. Wang, B. Zhang, and Y. J. Li, "Optimization of bolt-grouting time for soft rock roadway," *Rock and Soil Mechanics*, vol. 33, no. 5, pp. 1395–1402, 2012.

[29] L. Ma, F. Yang, H. Xu, and Z. Xie, "Post-yield properties of rock salt using the concept of mobilized strength components and the dilation angle," *Geotechnical and Geological Engineering*, vol. 35, no. 6, pp. 2841–2849, 2017.

[30] X. Zhu, L. Tang, and H. Tong, "Effects of high-frequency torsional impacts on rock drilling," *Rock Mechanics and Rock Engineering*, vol. 47, no. 4, pp. 1345–1354, 2014.